Electronic Supplementary Information for

Boosting solar cell performance during highly thermo- and photo-stable asymmetric perylene diimide dimeric acceptors by selenium-annulation at the outside bay position

Junfeng Tong*[,a,‡], Jiayu Fang[a,‡], Lili An[b], Youzhi Huo[c], Fushui Di[a], Pengzhi Guo[a], Chunyan Yang[a], Zezhou Liang[d], Jianfeng Li[a], Yangjun Xia*[,a]

[a]Gansu Provincial Engineering Research Center for Organic Semiconductor Materials and Application Technology, School of Materials Science and Engineering, Lanzhou Jiaotong University, Lanzhou, 730070, China.

[b]School of Chemical Engineering, Northwest Minzu University, Lanzhou 730030, China

[c]Harbin Station, China Railway Harbin Group Co., Ltd., Harbin, 150010, China

[d]Key Laboratory for Physical Electronics and Devices of the Ministry of Education & Shaanxi Key Lab of Information Photonic Technique, School of Electronics and Information Engineering, Xi′an Jiaotong University, Xi′an, 710049, China.

*Corresponding Author: E-mail: tongjunfeng139@163.com; xiayangjun2015@126.com

‡These authors contributed equally to this work.

1. Experimental Section.

1.1. Measurement and characterization

^{1}H NMR spectra was measured on a Bruker 500 MHz Avance NEO spectrometer (Rheinstetten, Germany), with tetramethylsilane (TMS) as the internal reference. The chemical shifts (δ) were recorded in units of ppm and their splitting patterns were designed as s (singlet), d (doublet), t (triplet), m (multiplet), and br (broaden). Melting points were obtained on a microscopic melting point apparatus (Beijing Taike), and the temperature gauge was uncorrected. HR-MALDI-TOF mass spectra were determined on Bruker solariX 9.4 Tesla Fourier Transform Mass Spectrometer. C, H and N elemental analyses (EAs) were carried out on a Vario EL Elemental Analysis Instrument (Elementar Co.). TGA curves were collected on a TGA 2050 instruments (New Castle, DE, USA) at the heating rate of 10 ºC min^{-1} and under a N_2 flow rate (20 mL min^{-1}). UV-Vis absorption measurement was performed on a UV-1800 spectrophotometer (Shimadzu, Kyoto, Japan). Thin film X-ray diffraction (XRD) was recorded on a PANalytical X′Pert PRO diffractometer equipped with a rotating anode (Cu *K*α radiation, λ = 1.54056 Å). The electrochemical properties of nonfullerene small molecules films were measured on a CHI600D electro-chemical instrument (Shanghai Chenhua, Shanghai, China) in anhydrous CH_3CN at a scan rate of 100 $mV \cdot s^{-1}$ under N_2. Tetra(n-butyl)ammonium hexafluorophosphate (Bu_4NPF_6) (0.1 $mol \cdot L^{-1}$) was utilized as the electrolyte. A three-electrode cell was used in all experimental, wherein glassy carbon electrode coated by polymer film, platinum wire and $Ag/AgNO_3$ (0.01 M of $AgNO_3$ in CH_3CN) electrode were used as the working, counter and reference electrode, respectively. The potential of $Ag/AgNO_3$ reference electrode was calibrated by the ferrocene/ferrocenium couple (Fc/Fc^+), whose energy level was –4.80 eV. Note that small molecule thin films were obtained by dropcasting 1 μL small molecules material chlorobenzene solution with the concentration of 1 $mg \cdot mL^{-1}$ onto the glass carbon electrode, and then dried in the air. Atomic force microscopy (AFM) images were acquired on an MFP-3D-SA (Asylum Research, Santa Barbara, CA, USA) in a tapping mode. The imaging and analysis were conducted using a field emission scanning electron microscope (Zeiss GeminiSEM 500) connected to an Oxford UltimMax65eds spectrometer.

1.2. Syntheses

1.2.1. Synthesis of [1,12-*b*,*c*,*d*]thiophene-*N*,*N*′-bis(2-hexyldecyl)perylene diimide (TPDI)

Under Ar, sulfur powder (72.0 mg, 2.262 mmol) was added into 25 mL double-neck

flask involving 10 mL *N*-methylpyrrolidone (NMP), the mixture was stirred at 70 ºC for 0.5 h. Then, PDI-HD-NO_2 (200 mg, 0.226 mmol) was added the above reaction mixture and heated up to 190 ºC. This reaction mixture was vigorously stirred for about 3 h until the disappearance of PDI-HD-NO_2 checked by TLC. After cooling, the mixture was poured into 200 mL 2 mol L^{-1} HCl solution, then the precipitate was collected through reduced-pressure filtration. The crude solid was extracted with CH_2Cl_2, following washed with H_2O, and then dried with anhydrous Na_2SO_4. Eventually, purifying the crude product *via* column chromatography (CC) using mixed solvent PE:CH_2Cl_2 (1:3) as an eluent produced the 132.5 mg orange solid as TPDI (Yield = 67%). M. p. 257~259 ℃. ^{1}H NMR (500 MHz, $CDCl_3$), δ (ppm): 8.96 (s, 2H, H of PDI), 8.58 (d, ^3J = 8.0 Hz, 2H, H of PDI), 8.48 (d, ^3J = 8.0 Hz, 2H, H of PDI), 4.30–4.28 (d, ^3J = 7.0 Hz, 4H, N–CH_2–), 2.03 (br, 2H, >CH–), 1.40–1.15 (m, 48H, –CH_2–), 0.85–0.80 (m, 12H, –CH_3). Elemental Anal. Calcd for $C_{56}H_{72}N_2O_4S$: C, 77.38%; H, 8.35%; N, 3.22%. Found, C, 77.22%; H, 8.27%; N, 3.35%.

1.2.2. Synthesis of 6-bromo-[1,12-*b*,*c*,d]thiophene-*N*,*N*′-bis(2-hexyldecyl)perylene diimide (TPDIBr)

In the 50 mL round-bottomed flask, TPDI (100.0 mg, 0.115 mmol) dissolved in 25 mL CH_2Cl_2, liquid bromine (1.29 g, 8.05 mmol) and $FeCl_3$ (100.0 mg, 0.616 mmol) was gradually added. This reaction mixture stirred at room temperature (RT) under dark and lasted for 5 h. The excess liquid bromine was removed by using saturated Na_2SO_3 solution. After removing the solvent, the crude product was purified by silica gel CC with PE:CH_2Cl_2 (1:2) mixed solvent as eluent to obtain the 68.3 mg TPDIBr as orange solid (Yield = 63%). M. p. 192~194 ℃. ^{1}H NMR (500 MHz, $CDCl_3$), δ (ppm): 9.95 (d, ^3J = 8.5 Hz, 1H, H of PDI), 9.03 (s, 1H, H of PDI), 8.99 (s, 1H, H of PDI), 8.78 (s, 1H, H of PDI), 8.61 (d, ^3J = 8.5 Hz, 1H, H of PDI), 4.22–4.16 (m, 4H, N–CH_2–), 2.06–2.01 (br, 2H, >CH–), 1.40–1.15 (m, 48H, –CH_2–), 0.86–0.81 (m, 12H, –CH_3). Elemental Anal. Calcd for $C_{56}H_{71}BrN_2O_4S$: C, 70.94%; H, 7.55%; N, 42.95%. Found, C, 70.82%; H, 7.44%; N, 5.03%.

1.2.3. Synthesis of [1,12-*b*,*c*,*d*]selenophene-*N*,*N*′-bis(2-hexyldecyl)perylene diimide (SePDI)

The Se-annulation procedure of SePDI was similar to that of TPDI, except for using selenium powder to replace sulfur powder. The target product was obtained as 135.4 mg of orange solid (Yield = 65%). M. p. 235~237 ℃. ^{1}H NMR (500 MHz, $CDCl_3$), δ (ppm): 9.04 (br, 2H, H of PDI), 8.60 (br, 2H, H of PDI), 8.51 (br, 2H, H of PDI), 4.25 (d, ^3J = 7.5 Hz, 4H, N–CH_2–), 2.03 (m, 2H, >CH–), 1.44–1.20 (m, 48H, –CH_2–) 0.85–0.82 (m, 12H, –CH_3).

Elemental Anal. Calcd for $C_{56}H_{72}N_2O_4Se$: C, 73.42%; H, 7.92%; N, 3.06%. Found, C, 73.33%; H, 7.81%; N, 3.15%.

1.2.4. Synthesis of 6-bromo-[1,12-*b*,*c*,*d*]selenophene-*N*,*N*′-bis(2-hexyldecyl)perylene diimide (SePDIBr)

The brominating procedure of SePDIBr was similar to that of TPDIBr. The 66.3 mg title compound was obtained as orange solid (Yield = 61%). M. p. 222~224 ℃. ^{1}H NMR (500 MHz, $CDCl_3$), δ(ppm): 9.79 (d, ^3J = 8.5 Hz, 1H, H of PDI), 9.01 (s, 1H, H of PDI), 8.96 (s, 1H, H of PDI), 8.72 (s, 1H, H of PDI), 8.51 (d, ^3J = 8.5 Hz, 1H, H of PDI), 4.20–4.14 (m, 4H, N–CH_2–), 2.13–2.00 (br, 2H, >CH–), 1.45–1.21 (m, 48H, –CH_2–), 0.87–0.82 (m, 12H, –CH_3). Elemental Anal. Calcd for $C_{56}H_{71}BrN_2O_4Se$: C, 67.59%; H, 7.19%; N, 2.82%. Found, C, 67.47%; H, 7.12%; N, 2.93%.

1.2.5. Synthesis of 1-(4,4,5,5-tetramethyl-1,3,2-dioxaborolan-2-yl)-*N*,*N*′-bis(2-hexyldecyl)-perylene diimide (PDI-Bpin)

Under the Ar atmosphere, PDI-HDBr (70.0 mg, 0.076 mmol), K_2HPO_4 (66.2 mg, 0.38 mmol) and 5 mL ortho-xylene were in sequence added into a 25 mL double-necked vial. After purging the above reaction solution for 10 min with Ar, bis(pinacolato)diboron (57.9 mg, 0.228 mmol) and Pd(dppf)Cl_2 (5.7 mg, 0.0076 mmol) were added. The resulting solution kept refluxing for about 18 h. This solution was poured into H_2O and extracted with CH_2Cl_2. Following, it was washed with H_2O and then dried by anhydrous Na_2SO_4. After removing the solvent, the obtained crude product was purified by CC using PE:CH_2Cl_2 (1:2) mixed solvent as an eluent to produce 31.1 mg of PDI-Bpin as the dark-red solid. (Yield = 42%). M. p. 212~214 ℃. ^{1}H NMR (500 MHz, $CDCl_3$), δ (ppm): 8.76 (s, 1H, H of PDI), 8.62–8.60 (m, 2H, H of PDI), 8.55–8.51 (m, 3H, H of PDI), 8.28 (d, ^3J = 8.0 Hz, 1H, H of PDI), 4.15–4.12 (m, 4H, N–CH_2–), 2.00 (br, 2H, >CH–), 1.50 (s, 12H, –CH_3 of Bpin), 1.45–1.21 (m, 48H, –CH_2–), 0.86–0.83 (m, 12H, –CH_3 of *N*-alkyl). Elemental Anal. Calcd for $C_{62}H_{85}BN_2O_6$: C, 77.15%; H, 8.88%; N, 2.90%. Found, C, 77.01%; H, 8.72%; N, 2.99%.

1.3. Fabrication of Organic solar cell and mobility characterization

Indium tin oxide (ITO) coated glass substrates were washed by a wet-cleaning process inside an ultrasonic bath, with de-ionized water, acetone, de-ionized water and isopropanol in turn. After drying under nitrogen flow, the substrates were treated with oxygen plasma for 6 min, then a thin layer of poly(3,4-ethylenedioxythiophene):poly(styrene-sulfonate)

(PEDOT:PSS, ca. 40 nm, Clevios PVP Al4083) was spin-coated onto the ITO substrates and annealed at 160 ºC for 20 min. After that the substrates were transferred into a nitrogen-filled glove box and the active layer was prepared. The active layer, with a thickness in the 90–110 nm range, was deposited on top of the PEDOT:PSS layer by spin-casting from CB solution containing PTB7-Th:**PDI-TPDI** (w/w; 1:1.2, 1:1 and 1.2:1) and PTB7-Th:**PDI-SePDI** (w/w; 1:1.5, 1:1.8 and 1:2), respectively. The thickness of the active layer was verified by a surface profilometer (DektakXT, Bruker). Then, an ultrathin layer of PDINO (1.0 mg·mL^{-1} in methanol) was spin-coated on the active layer. Finally, the Al layer (~100 nm) as the cathode was thermally evaporated under a vacuum pressure of 10^{-4} Pa. Moreover, the all effective device area in this work was 0.1 cm^2, which was ascertained by a shadow mask. The thickness values of the evaporated Al were monitored by a quartz crystal thickness/ratio monitor (SI-TM206, Shenyang Sciens Co.). The PCEs of the resulting PSCs were measured under 1 sun, AM 1.5 G (Air mass 1.5 global) condition using a solar simulator (XES-70S1, San-EI Electric Co.) with irradiation of 100 mW·cm^{-2}. The current density-voltage (*J*-*V*) characteristics were recorded with a Keithley 2400 source-measurement unit. The spectral responses of the devices were measured with a commercial external quantum efficiency (EQE)/incident photon to charge carrier efficiency (IPCE) setup (7-SCSpecIII, Beijing 7-star Opt. In. Co.) equipped with a standard Si diode.

The electron-only device were prepared with a diode configuration of ITO/ZnO/ PTB7-Th:**PDI-TPDI** or PTB7-Th:**PDI-SePDI**/PDINO/Al, respectively. The device characteristics were extracted by modeling the dark current under an applied forward bias. The mobilities of active layers were extracted by fitting the current-voltage curves using the Mott-Gurney relationships (space-charge-limited current, SCLC). The field dependent SCLC behavior can be expressed as: $J = \frac{9}{8}\varepsilon_0\varepsilon_r\mu\frac{V^2}{L^3}$. Where J stands for the current density, ε_0 is the permittivity of free space (8.85×10^{-12} F·m^{-1}), ε_r is the relative permittivity of the transport medium (3 is a typical value for organic semiconductors), μ is the zero-field mobility, L is the thickness of the active layer, and effective voltage $V = (V_{appl} - V_{bi})$, where V_{appl} is the applied voltage to the device and V_{bi} is the built-in voltage. By linearly fitting $J^{1/2}$ with V, the mobilities were extracted from the slope and L: $\mu = \frac{slope^2 \times 8L^3}{9\varepsilon_0\varepsilon_r}$.

1.4. Surface energy calculation [S1,S2]

The surface tension (γ) can be evaluated using the Wu model, *via* Equations (1), (2), and (3), on the basis of the measured contact angles (θ) information.

$$\gamma_{\mathrm{water}}(1+cos\theta_{\mathrm{water}})=\frac{4\gamma^{\mathrm{d}}_{\mathrm{water}}\gamma^{\mathrm{d}}}{\gamma^{d}_{\mathrm{water}}+\gamma^{\mathrm{d}}}+\frac{4\gamma^{\mathrm{p}}_{\mathrm{water}}\gamma^{\mathrm{p}}}{\gamma^{\mathrm{p}}_{\mathrm{water}}+\gamma^{p}} \quad (1)$$

$$\gamma_{\mathrm{EG}}(1+\cos\theta_{\mathrm{EG}})=\frac{4\gamma^{\mathrm{d}}_{\mathrm{EG}}\gamma^{\mathrm{d}}}{\gamma^{\mathrm{d}}_{\mathrm{EG}}+\gamma^{\mathrm{d}}}+\frac{4\gamma^{\mathrm{p}}_{\mathrm{EG}}\gamma^{\mathrm{p}}}{\gamma^{\mathrm{p}}_{\mathrm{EG}}+\gamma^{\mathrm{P}}} \quad (2)$$

$$\gamma=\gamma^{\mathrm{d}}+\gamma^{\mathrm{p}} \quad (3)$$

Where, γ is the surface energy of the studied semiconductor; γ^{d} and γ^{p} are the dispersion and polar components of γ; γ_i is the total surface energy of the i material (i = water or ethylene glycerol (EG)); γ_i^{d} and γ_i^{p} are the dispersion and polar components of γ_i; and θ is the droplet contact angle (water or EG) on the semiconductor film. Flory-Huggins interaction parameter χ^{D-A}, which is a parameter to evaluate the interaction between polymer donor PTB7-Th and the studied non-fullerene acceptors, based on this, the miscibility of the two components can be objectively judged. The smaller the difference of surface energy between donor and acceptor, the lower the value of χ^{D-A} and the better the miscibility.

2. **Supplementary Figures and Tables**

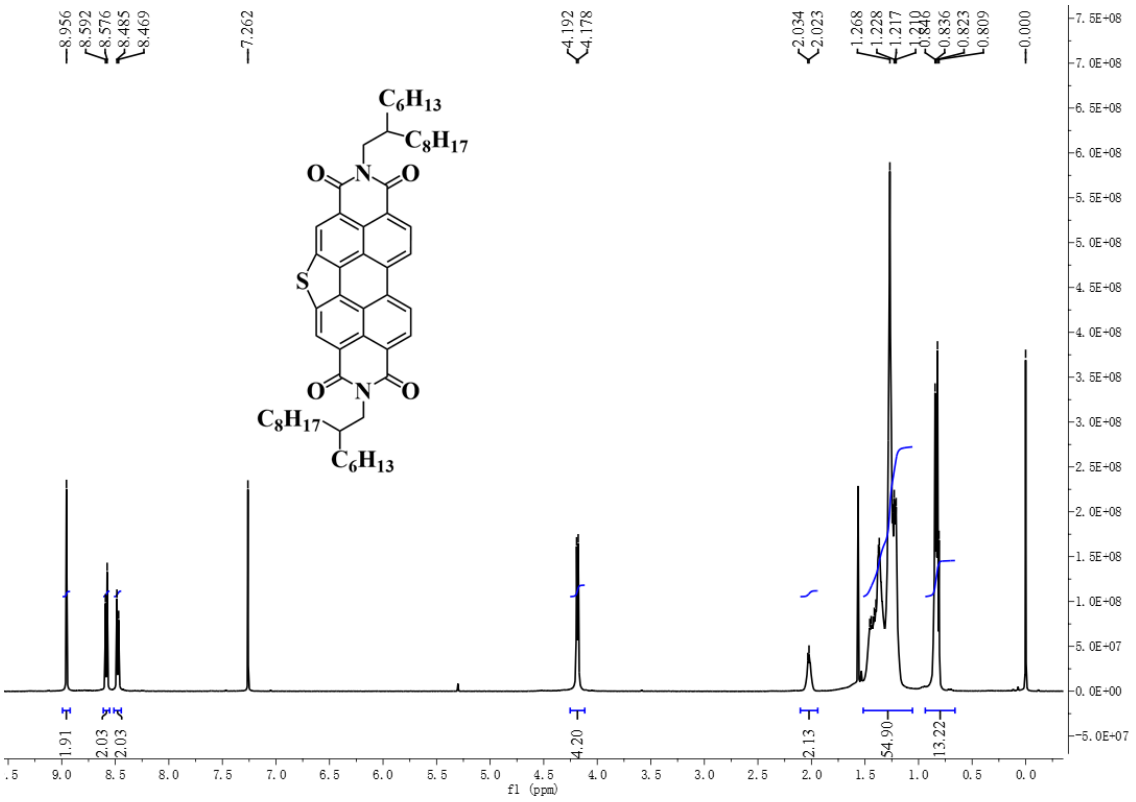

Fig. S1. The ^{1}H NMR spectrum of **TPDI** in $CDCl_3$.

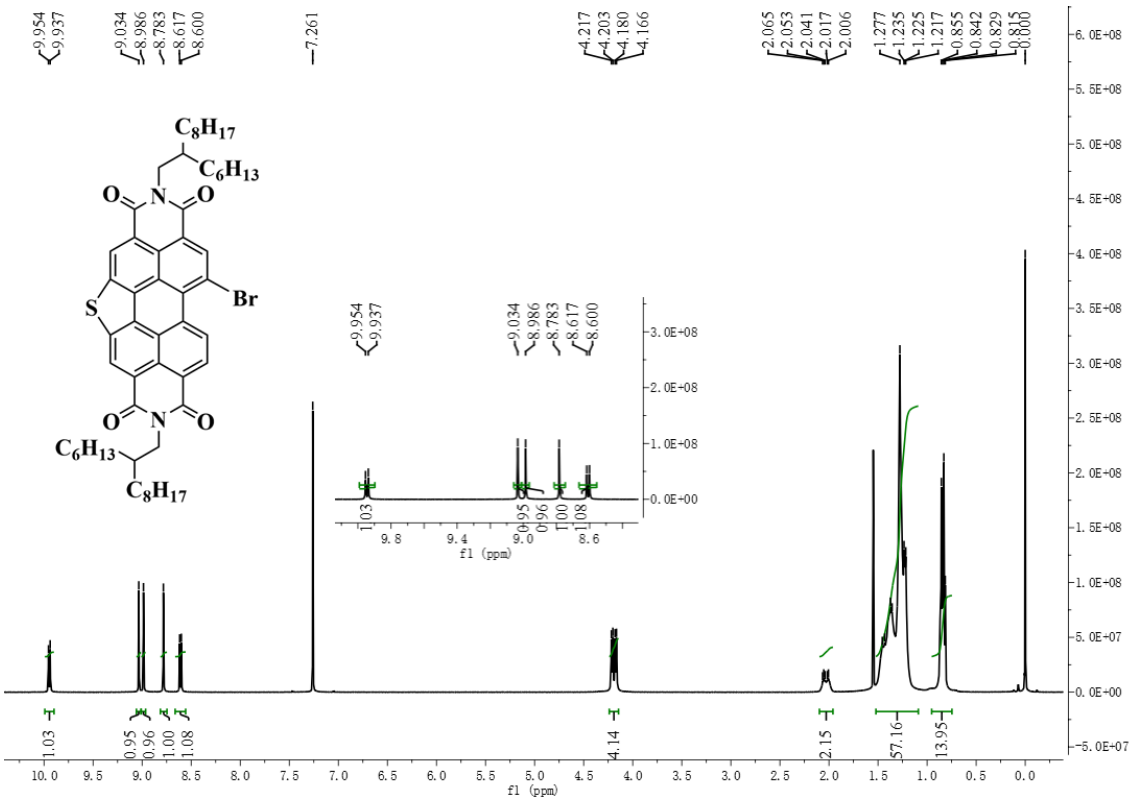

Fig. S2. The ^{1}H NMR spectrum of **TPDIBr** in $CDCl_3$.

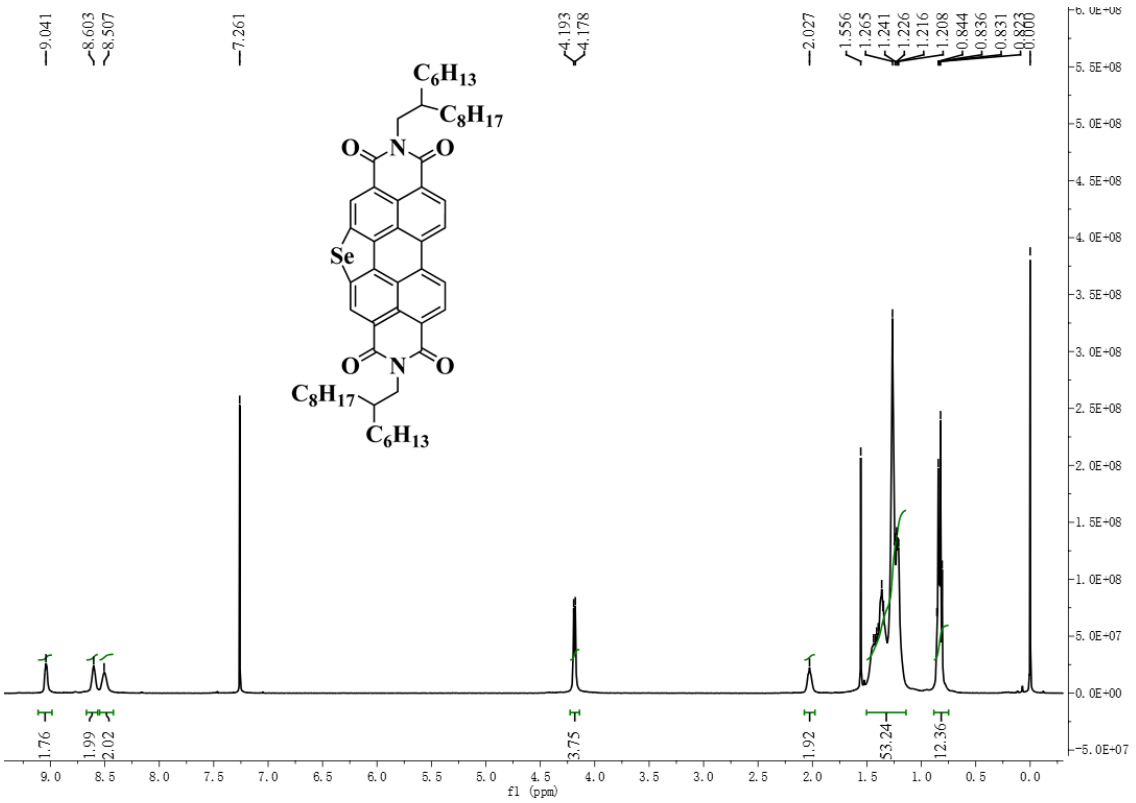

Fig. S3. The ^{1}H NMR spectrum of **SePDI** in $CDCl_3$.

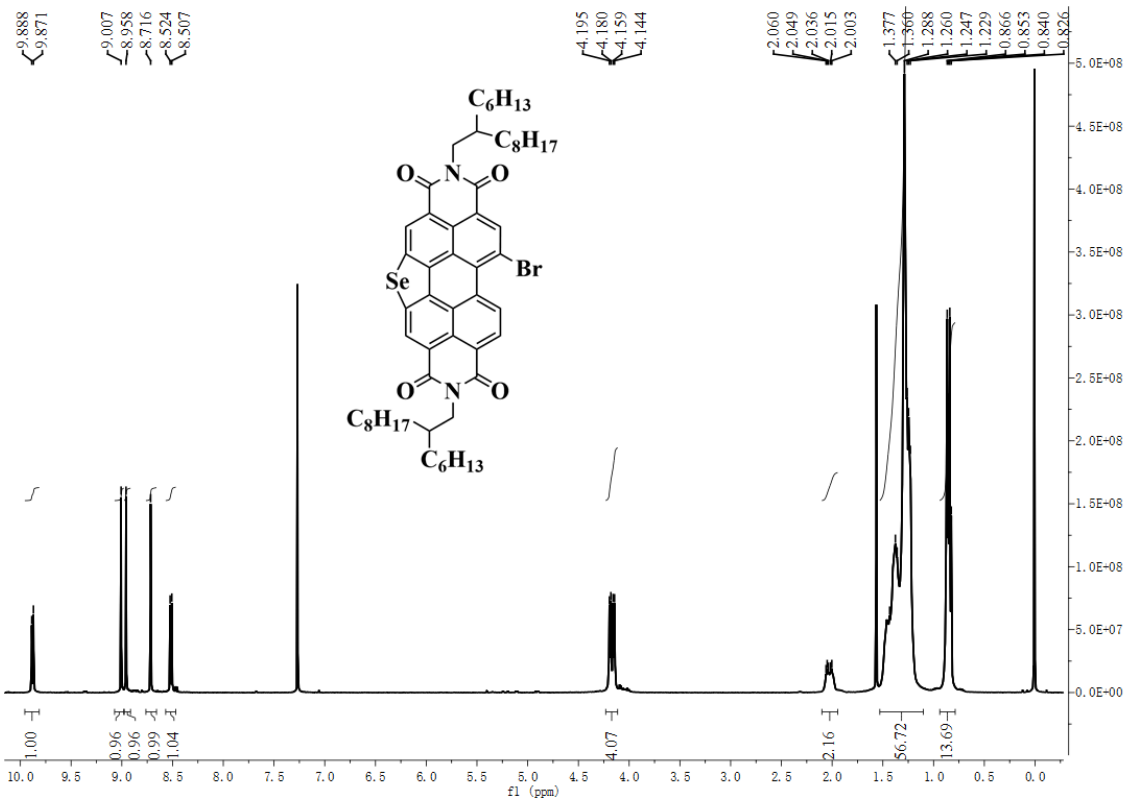

Fig. S4. The ^{1}H NMR spectrum of **SePDIBr** in $CDCl_3$.

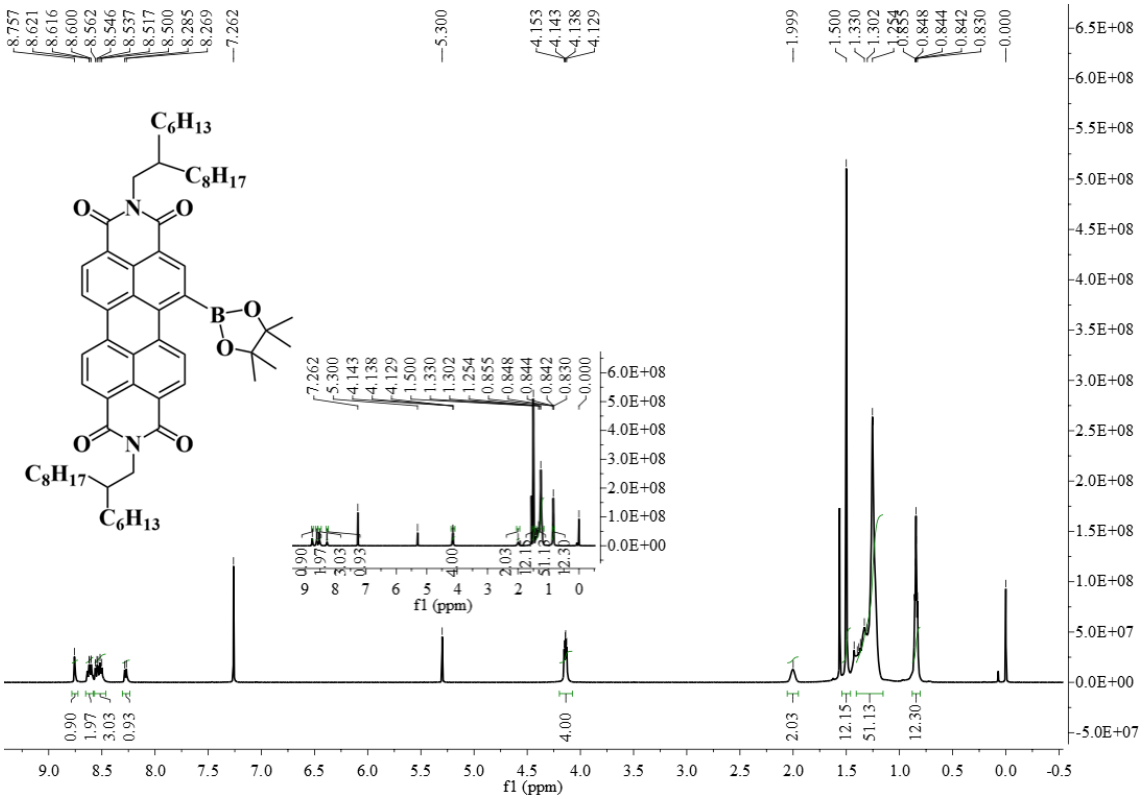

Fig. S5. The ^{1}H NMR spectrum of **PDI-Bpin** in $CDCl_3$.

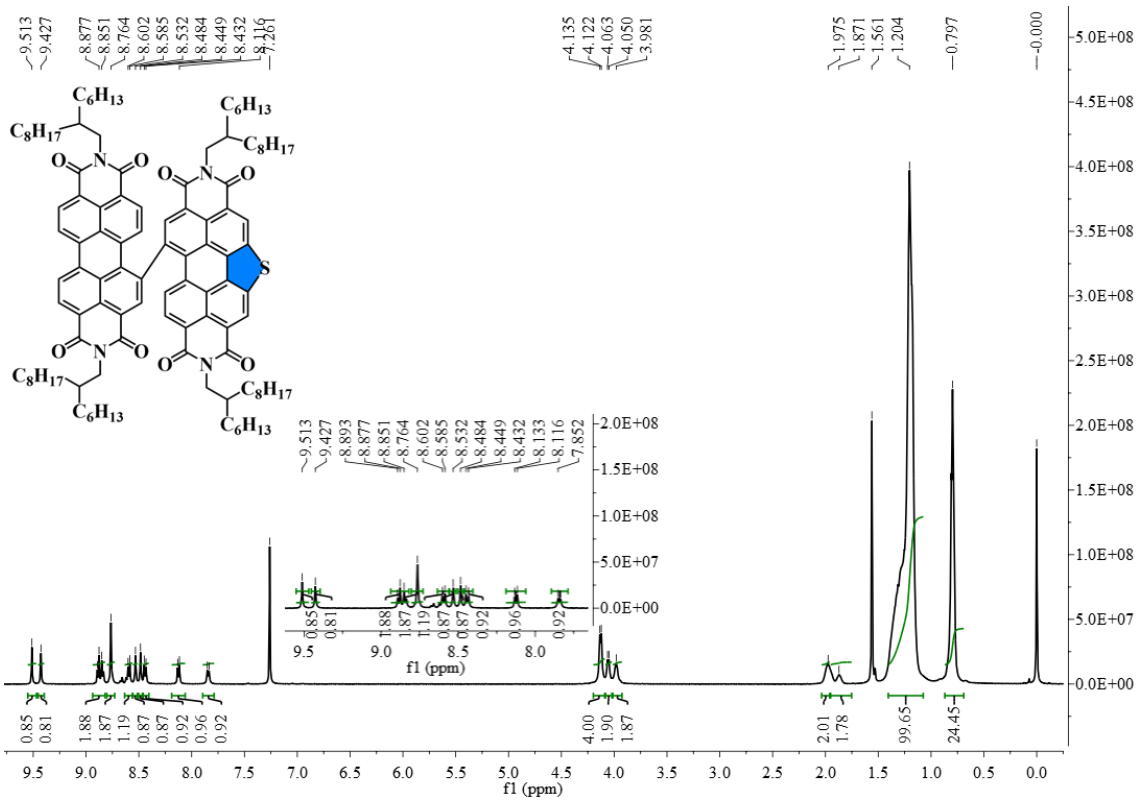

Fig. S6. The ^{1}H NMR spectrum of **PDI-TPDI** in $CDCl_3$.

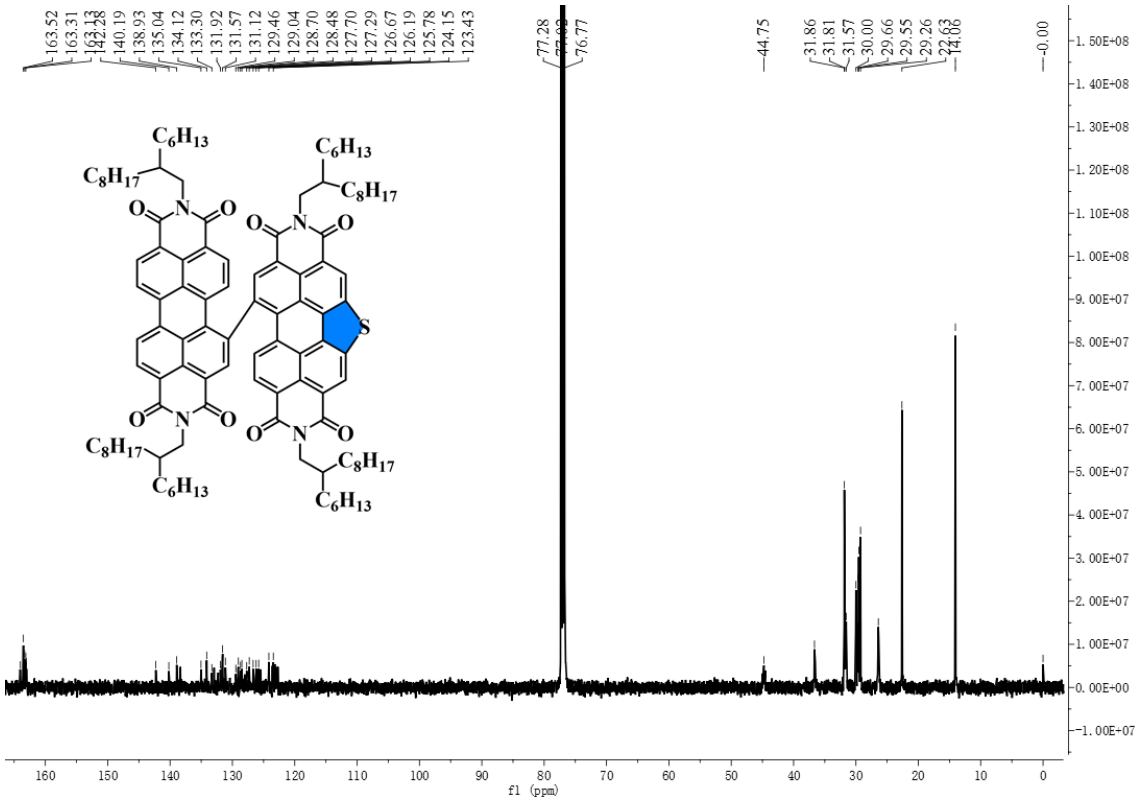

Fig. S7. The ^{13}C NMR spectrum of **PDI-TPDI** in $CDCl_3$.

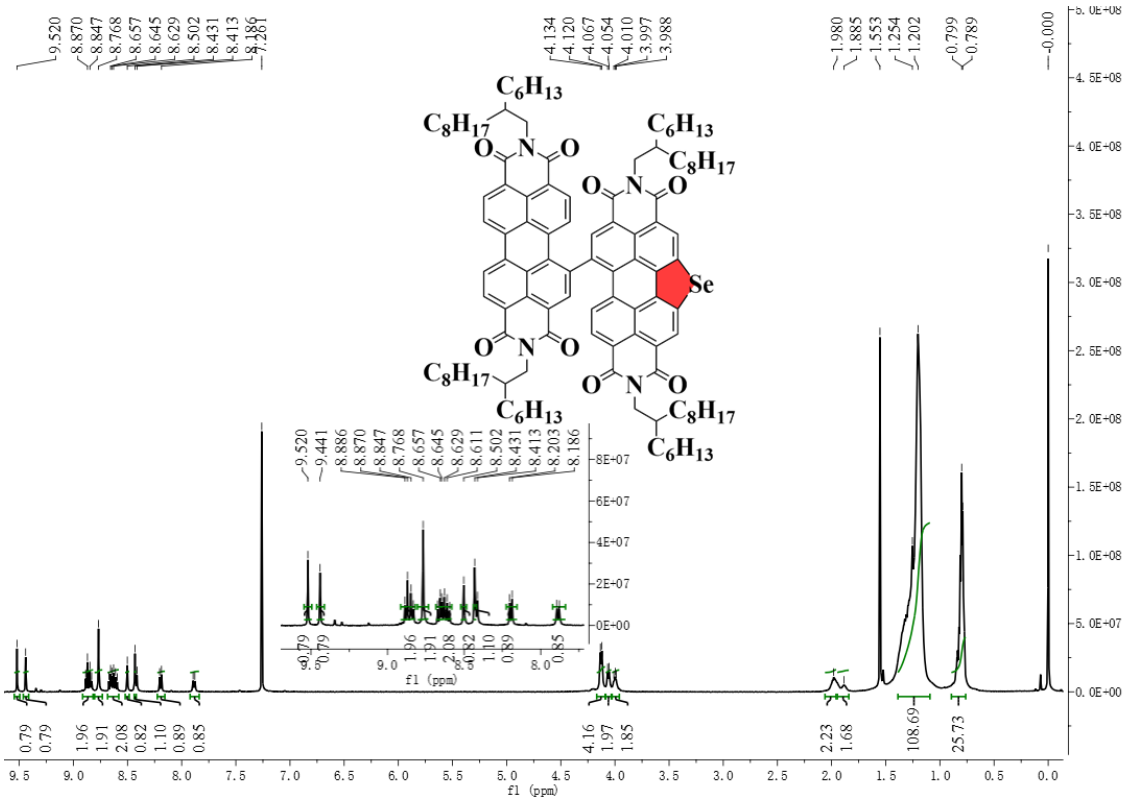

Fig. S8. The ^{1}H NMR spectrum of **PDI-SePDI** in $CDCl_3$.

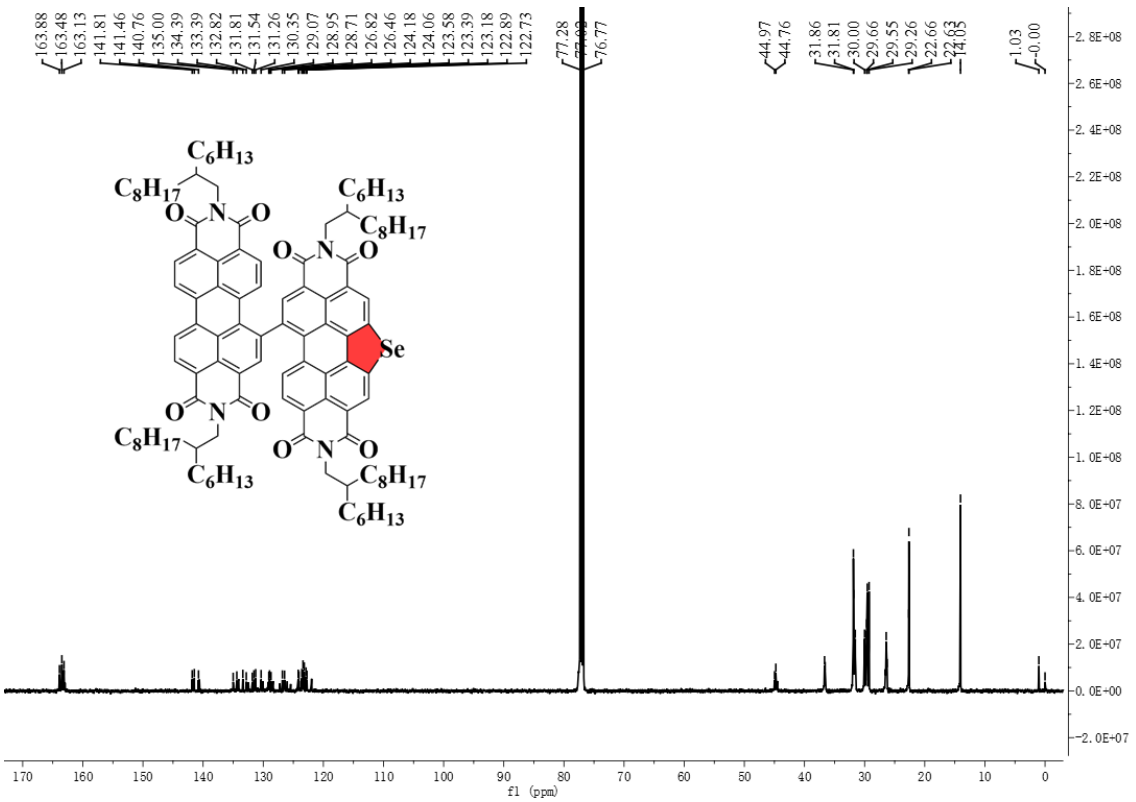

Fig. S9. The ^{13}C NMR spectrum of **PDI-SePDI** in $CDCl_3$.

Table S1. Yields, decomposed temperature and absorption coefficients for **PDI-TPDI** and **PDI-SePDI**.

Acceptors	colour	Yield (%)	T_d (°C)	ε_{soln} (L mol^{-1} cm^{-1})	λ_{em}^{sol} (nm)	λ_{em} (nm)
PDI-TPDI	red	25	426	6.71×10^4 (λ = 503 nm)	584	628
PDI-SePDI	reddish brown	23	409	5.52×10^4 (λ = 526 nm)	532, 575	634

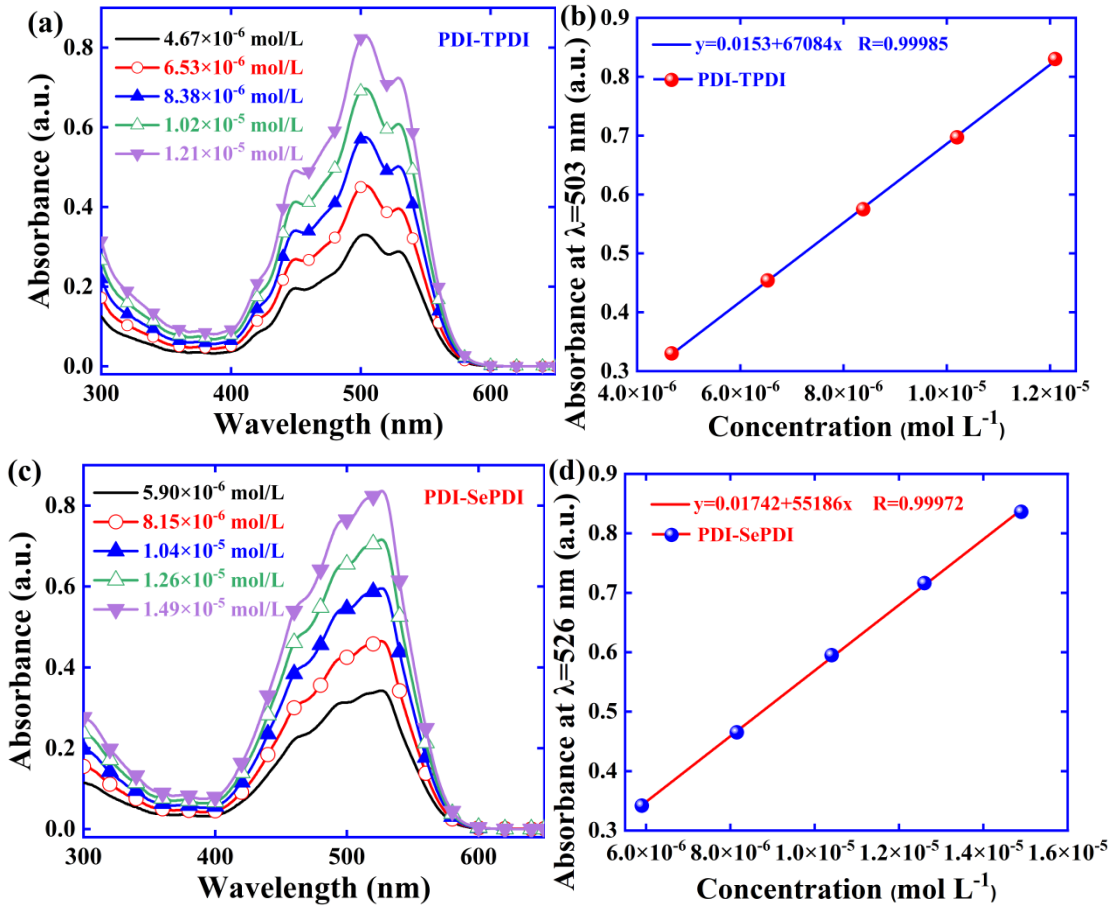

Fig. S10. UV-vis absorption spectra of **PDI-TPDI** and **PDI-SePDI** dissolved in CB at varied concentrations and calculation of molar absorption coefficient.

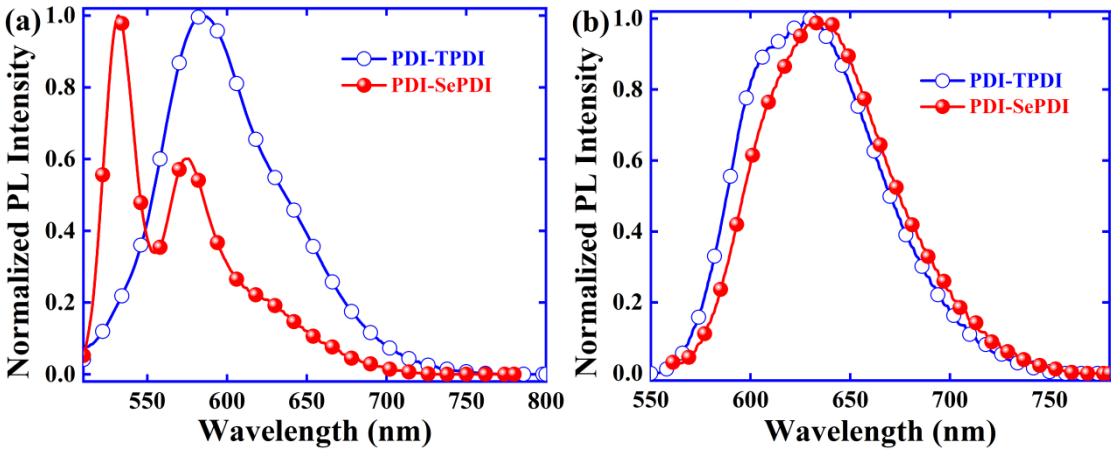

Fig. S11. Fluorescence spectra of **PDI-TPDI** and **PDI-SePDI** in CH_2Cl_2 solution (a) and film (b).

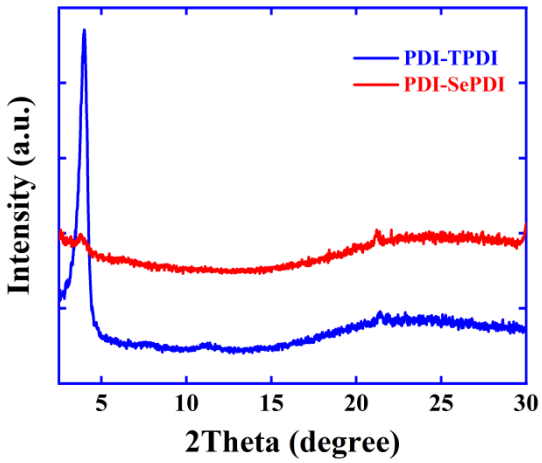

Fig. S12. XRD patterns for **PDI-TPDI** and **PDI-SePDI** films.

Table S2. The dihedral data of model molecules **PDI-TPDI** and **PDI-SePDI**.

Model Molecules	Structure	Dihedral angle (deg)
PDI-TPDI	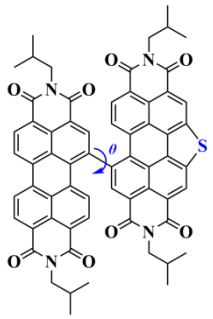	θ_1 = 107.98
PDI-SePDI	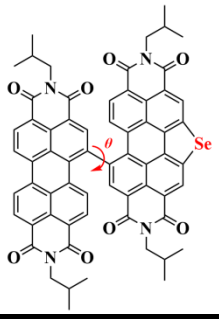	θ_1 = 108.19

Table S3. Molecular surface area, MPI extreme value of ESP and total average ESP of model molecules **PDI-TPDI and PDI-SePDI** and $(TB7\text{-}Th)_2$ simplified from donor PTB7-Th.

model molecules	overall surface area (Å^2)	MPI (kcal/mol)	minimal value (kcal/mol)	maximal value (kcal/mol)	overall average value (kcal/mol)
PDI-TPDI	927.35	8.96	–30.25	34.37	2.85
PDI-SePDI	931.09	8.90	–30.46	34.32	2.71
$(TB7\text{-}Th)_2$	1385.25	7.64	–37.97	19.57	–1.61

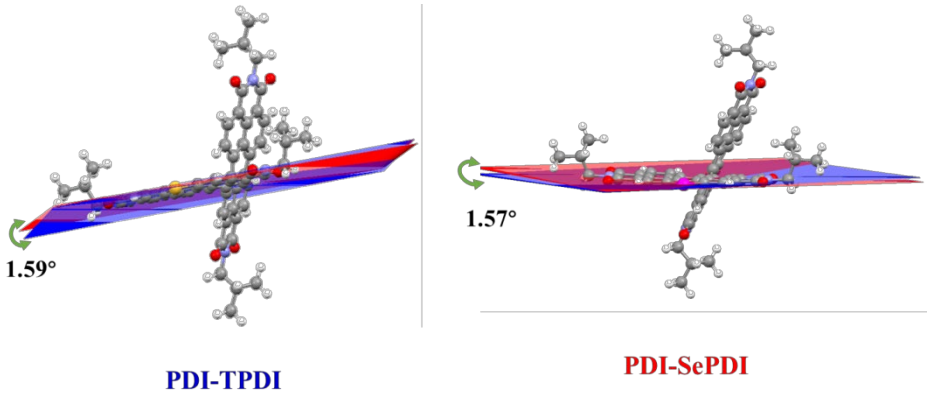

Fig. S13. Dihedral angle between PDI ring and heterocyclic ring in the heteroatom-annulated PDI subunit for **PDI-TPDI** and **PDI-SePDI**.

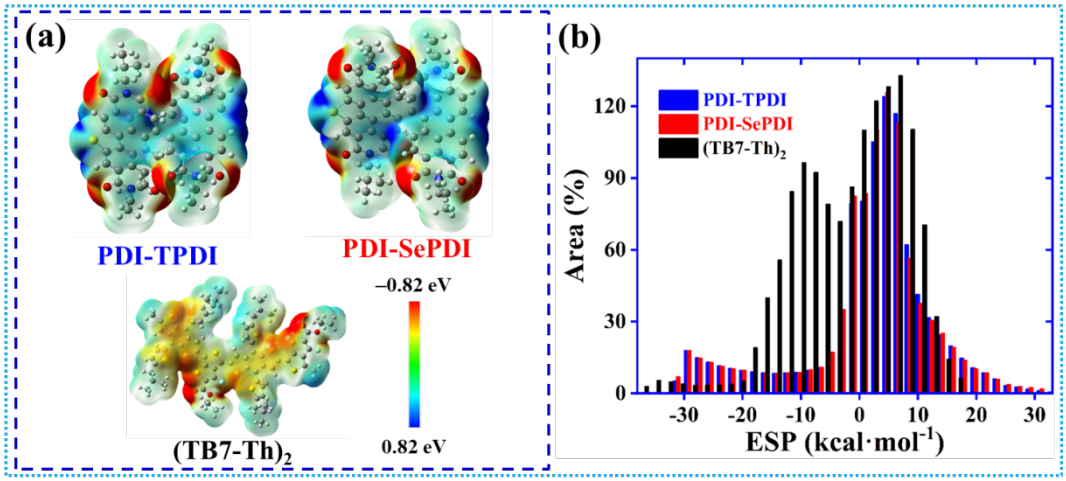

Fig. S14. Molecular ESP distribution (a) and ESP area distribution (b) of model molecules **PDI-TPDI**, **PDI-SePDI** and $(TB7\text{-}Th)_2$ simplified from donor PTB7-Th.

Table S4. The photovoltaic performance of devices with different blend weight ratio, and 3%(volume) DIO and thermal annealing,.

Active layer	Condition	V_{OC} (V)	J_{SC} (mA·cm^{-2})	*FF* (%)	PCE (%)[b]
PTB7-Th: **PDI-TPDI**	1:1.2	0.71±0.02	6.57±0.15	41.28±0.25	1.94±0.08
	1:1	0.72±0.01	7.02±0.28	61.34±0.33	3.10±0.15
	1.2:1	0.70±0.01	5.04±0.14	47.95±0.25	1.70±0.11
	1:1/3%DIO	0.72±0.01	4.27±0.08	46.17±0.38	1.43±0.08
	1:1/TA[a]	0.72±0.01	9.39±0.12	50.11±0.43	3.39±0.23
PTB7-Th: **PDI-SePDI**	1:1.5	0.70±0.01	7.96±0.13	37.83±0.41	2.09±0.09
	1:1.8	0.71±0.01	10.73±0.32	45.83±0.37	3.50±0.11
	1:2	0.70±0.01	8.29±0.18	36.74±0.42	2.12±0.10
	1:1.8/3%DIO	0.70±0.01	5.20±0.13	56.73±0.45	2.07±0.05
	1:1.8/TA[a]	0.70±0.01	14.64±0.22	51.84±0.38	5.31±0.24

[a] Thermal annealing at 110 °C for 10 min.

[b] The average values of all device parameters obtained from 10 independent devices.

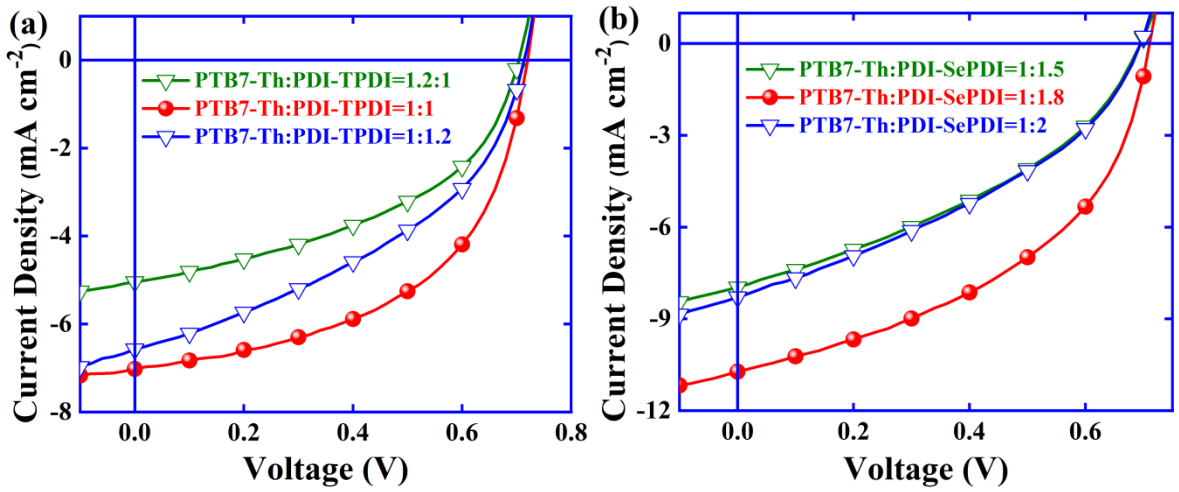

Fig. S15. The *J-V* curves for the devices with different blend weight ratio.

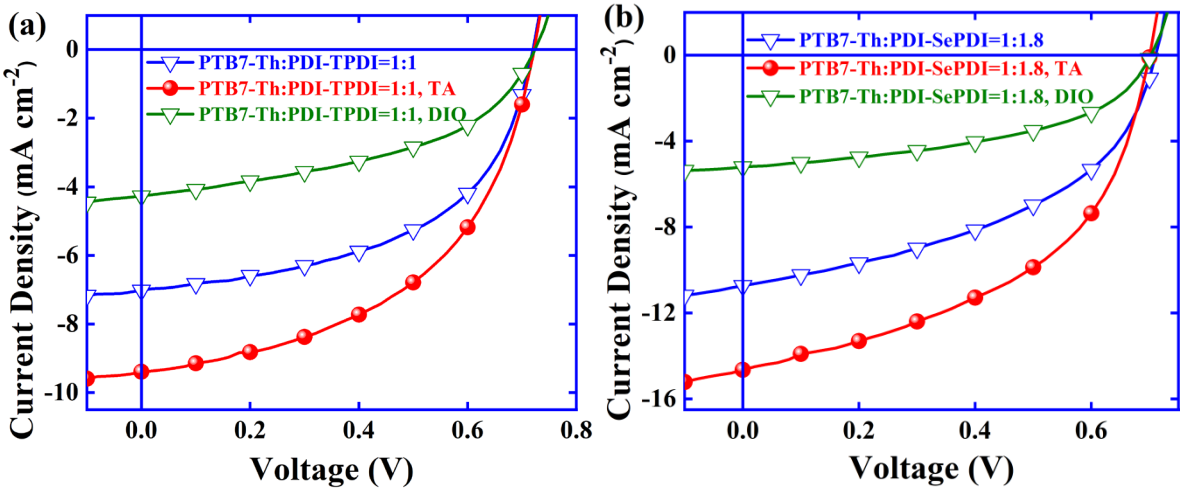

Fig. S16. The *J-V* curves for the devices using TA treatment and using 3%DIO solvent addictive.

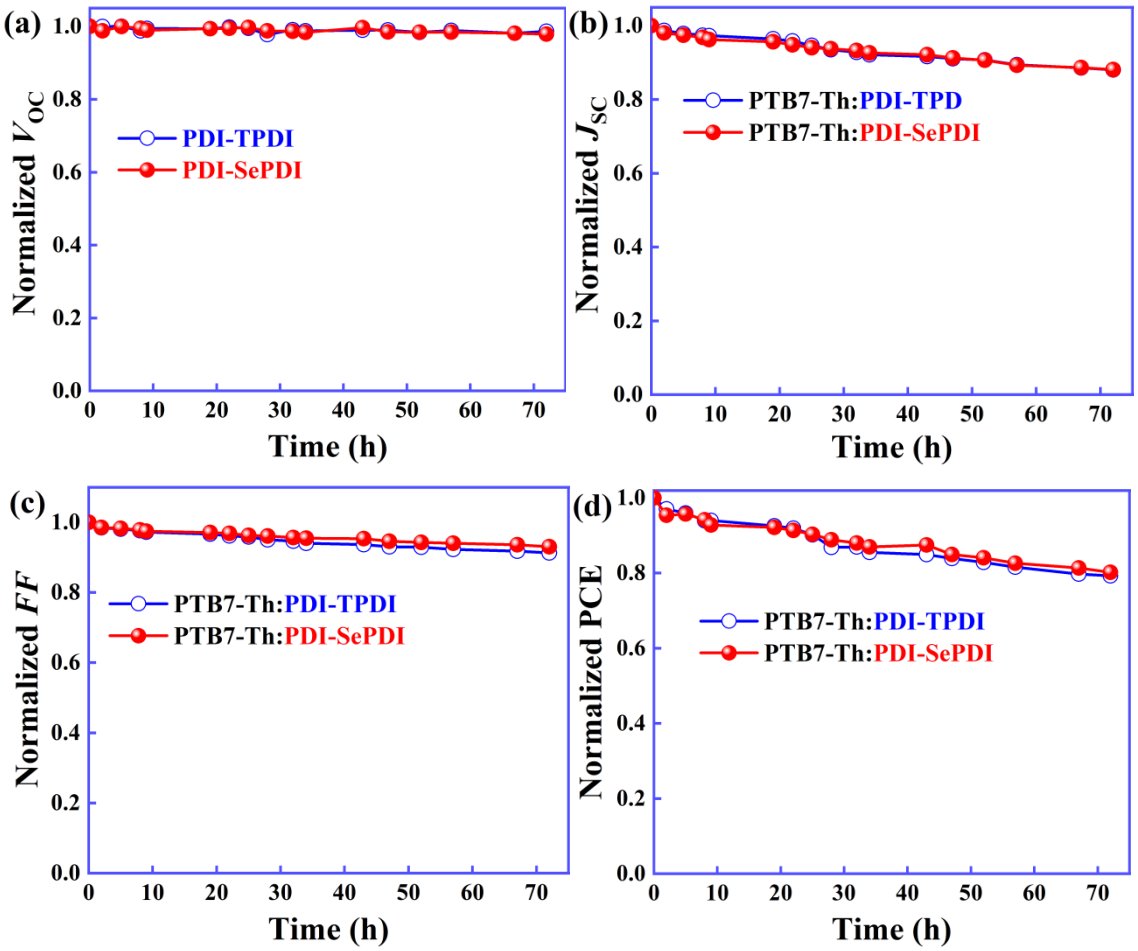

Fig. S17. The storage stability of **PDI-TPDI**- and **PDI-SePDI**-based devices.

Table S5. Electron mobility of PTB7-Th:**PDI-TPDI** and PTB7-Th:**PDI-SePDI**-based devices.

Active layer	Condition	Thickness (nm)	Slope	μ_e (cm^2 V^{-1} s^{-1})
PTB7-Th:**PDI-TPDI**	1:1/TA	100	6.09	1.24×10^{-5}
PTB7-Th:**PDI-SePDI**	1:1.8/TA	105	10.13	3.98×10^{-5}

Table S6. CA data of water and EG, surface tension and interaction parameters (χ) of donor PTB7-Th and asymmetric acceptors **PDI-TPDI** and **PDI-SePDI**.

Film	θ_{Water} (°)	θ_{EG} (°)	γ (mN m^{-1})	$\chi^{donor\text{-}acceptor}$
PTB7-Th	101.8	72.1	29.65	–
PDI-TPDI	103.9	80.3	20.53	0.863K
PDI-SePDI	106.5	80.2	23.47	0.361K

Reference

[S1] K.-H. Kim, H. Kang, H. J. Kim, P. S. Kim, S. C. Yoon, and B. J. Kim, *Chem. Mater.*, 2012, **24**, 2373−2381.

[S2] J. Comyn, *Int. J. Adhes. Adhes.*, 1992, **12**, 145–149.